PHILOSOPHICAL TRANSACTIONS OF THE ROYAL SOCIETY A MATHEMATICAL, PHYSICAL & ENGINEERING SCIENCES

Recent Progress in NMR Microscopy towards Cellular Imaging

Z. H. Cho, C. B. Ahn, S. C. Juh, J. M. Jo, R. M. Friedenberg, S. E. Fraser and R. E. Jacobs

Phil. Trans. R. Soc. Lond. A 1990 **333**, 469-475
doi: 10.1098/rsta.1990.0174

Recent progress in NMR microscopy towards cellular imaging

By Z. H. Cho[1,3], C. B. Ahn[1], S. C. Juh[1], J. M. Jo[3], R. M. Friedenberg[1], S. E. Fraser[2] and R. E. Jacobs[2]

[1] *Department of Radiological Sciences,* [2] *Department of Physiology and Biophysics, University of California, Irvine, California 92717, U.S.A.*

[3] *Department of Electrical Science, Korea Advanced Institute of Science, P.O. Box 150, Cheongyangni, Seoul, Korea*

Recent advances in NMR microscopy based on fundamental physical parameters and experimental factors are discussed. We consider fundamental resolution limits due to molecular diffusion and the experimental system bandwidth, as well as practical resolution limits arising from poor signal-to-noise ratio due to small imaging voxel size and finite line broadening due to signal attenuation brought about by diffusion. Several microscopic imaging pulse sequences are presented and applied to elucidating cellular imaging problems such as the cell lineage patterns in *Xenopus laevis* embryos. Experimental results obtained with 7.0 T NMR microscopy system are presented.

1. Introduction

The history of microscopy from optical microscopy to present-day scanning electron microscopy and the even more exotic proton and heavy ion microscopy suggests the importance of microscopy in both the physical and life sciences (Cho *et al.* 1978). NMR microscopy (House 1984; Lauterbur 1984; Aguayo *et al.* 1986; Cho *et al.* 1988) is an extension of NMR imaging with resolution improved down to a few micrometres. The major advantage of NMR microscopy is its non-invasive and non-ionizing nature together with an inherent high-resolution and high-contrast tomographic capability, which allows true non-invasive *in vivo* three-dimensional imaging.

In this paper, fundamental parameters in NMR microscopy at micrometre resolution are reviewed and theoretical resolution limits are examined as a function of diffusion, system bandwidth, and available gradient strength. The diffusion-dependent signal attenuation during the data acquisition period is also examined in terms of the line spread function. Other critical parameters such as the voxel-size-dependent signal-to-noise ratio (SNR) and main magnetic-field-strength-dependent SNR are analysed in conjunction with the existing 7.0 T NMR microscopy system. Several imaging pulse sequences optimized for NMR microscopy and *in vivo* localized microscopy using a gradient sub-encoding sequence are considered. Experimental results obtained with the 7.0 T microscopic imaging system are presented with particular emphasis on cellular imaging and *in vivo* localized microscopic imaging.

Phil. Trans. R. Soc. Lond. A (1990) **333**, 469–475
Printed in Great Britain

2. Review of the fundamental quantities in NMR microscopy

(a) Basic resolution limiting factors

Resolution limit by the bandwidth

The fundamental relation between spatial resolution and bandwidth can be derived from the basic imaging equation, which is given by $\Delta\phi_r^{min}/(\gamma G T_{acq})$, where γ is gyromagnetic ratio, G is gradient strength, T_{acq} is data acquisition time, and $\Delta\phi_r^{min}$ is a minimal detectable phase which is dependent on the reconstruction algorithm (Cho *et al.* 1988). For a given minimal detectable phase, resolution can be improved by increasing the gradient–data acquisition time product.

Resolution limit due to diffusion

Another important resolution-limiting factor is the molecular diffusion, which is proportional to the square root of the data acquisition time, i.e. $\sqrt{(\frac{2}{3}DT_{acq})}$. The above two resolution limiting factors are interrelated and are graphically shown in figure 1 as a function of data acquisition time.

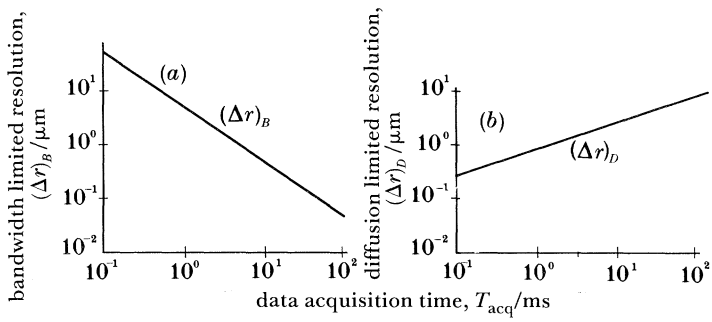

Figure 1. Bandwidth and diffusion limited resolution in NMR microscopy are plotted as a function of acquisition time. $D = 10^{-5}$ cm^2 s^{-1}, $G = 0.02$ T cm^{-1}. (*a*) $(\Delta r)_B = \pi/\gamma G T_{acq}$; (*b*) $(\Delta r)_D = \sqrt{(\frac{2}{3}DT_{acq})}$.

Line broadening due to diffusion

Another practical resolution-limiting factor is signal attenuation due to diffusion. This is due to the exponential decay of the diffusion-dependent signal amplitude resulting in a line or point spread function in the image domain (Ahn & Cho 1989). This line broadening can be a major resolution-degrading factor in micrometre resolution NMR microscopy.

(b) Other resolution limiting factors and compensation techniques

Voxel-size-dependent SNR

In addition to the fundamental limiting factors discussed in the previous section, NMR microscopy is seriously handicapped by poor SNR due to small voxel size. If the voxel dimension is d, the NMR signal intensity will be proportional to d^3 for a given RF coil. The detected signal intensity is, however, proportional to d^2 because of the increased RF coil sensitivity which is inversely proportional to the object dimension for the same filling factor. Since the dominant noise source in microscopic imaging is the coil thermal noise when the object size is small (Hoult & Lauterbur 1979), the overall SNR in microscopic imaging is more or less proportional to the

PHILOSOPHICAL TRANSACTIONS OF THE ROYAL SOCIETY A MATHEMATICAL, PHYSICAL & ENGINEERING SCIENCES

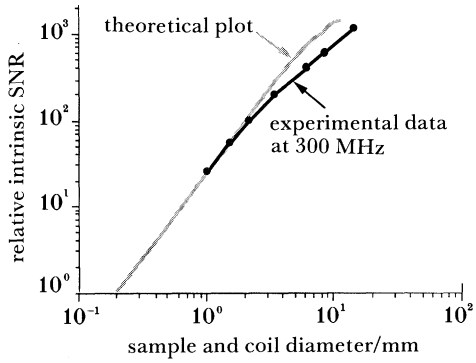

Figure 2. Experimental and calculated values of the SNR as a function of sample and coil diameter.

square of the voxel dimension. Both theoretically calculated values and experimentally measured intrinsic SNRs are shown in figure 2.

Avenues for further SNR enhancement in NMR microscopy

There are several avenues for the enhancement of SNR in NMR microscopic imaging. (i) Increase the main magnetic field strength. The SNR in NMR is believed to be improved in proportion to $B_0^{\frac{7}{4}}$ when the coil thermal noise is the major noise source (Hoult & Richards 1976). For example, the increase in main magnetic field from 0.5 T to 7.0 T will improve the SNR by a factor of more than 100. (ii) Reduction of sample induced noise will result in a decrease of overall noise in microscopic imaging. For example, SNR improvement in microscopic imaging is more than a factor of 10 compared with conventional whole body diagnostic imaging. (iii) There are also expected improvements in sensitivity by using a multiturn solenoidal coil instead of the conventional RF coil used in the whole body imaging system. (iv) In addition to the above physical factors, SNR can further be improved by the use of microscopy optimized imaging pulse sequences such as three-dimensional techniques and small tip angle driven equilibrium sequences with short repetition time, etc., as will be discussed in the next section. By combining the above techniques, the SNR in microscopic imaging at a few micrometres resolution appears possible and is a promising tool for many biological studies where imaging of a non-invasive nature is crucial.

3. Imaging methods in NMR microscopy

There are several proposed NMR microscopic imaging sequences, such as the diffusion effect reduced gradient echo (DRG) sequence, the driven equilibrium Fourier transform (DEFT) sequence, and the planar integral projection pulse sequence. Most of these methods use three-dimensional techniques to improve SNR further. To obtain a three-dimensional data-set within a reasonably short time (less than an hour), a short repetition time is usually necessary. As will be seen, localized microscopic imaging is also becoming important since many *in vivo* measurements require localization of the sample. The single most important physical parameter to be considered in microscopy is diffusion. It not only degrades resolution, but also causes serious intensity attenuation thereby lowering SNR. With this in mind, several imaging methods have been developed for NMR microscopy.

PHILOSOPHICAL TRANSACTIONS OF THE ROYAL SOCIETY A MATHEMATICAL, PHYSICAL & ENGINEERING SCIENCES

(*a*) *Driven equilibrium Fourier transform sequence*

The DEFT sequence is an NMR sensitivity enhancement technique suggested by Becker. In spite of the obvious advantages, there are several difficulties in the application of the DEFT sequence in imaging experiments, especially in the area of clinical applications where uniform and accurate RF excitation over the whole imaging volume is required. The small object volumes involved in NMR microscopy, however, allow uniform RF excitation by using multiturn solenoidal coils.

(*b*) *Modified small-tip-angle DEFT sequence*

The roles of T_1 and T_2 in the NMR contrast mechanism are well established in diagnostic NMR imaging. To obtain T_1 contrast, repetition time and inversion time, as well as excitation angle, are controlled in the conventional spin echo or inversion recovery sequence. Although the small-tip-angle method is not new and has been used in many gradient echo sequences, use of these methods have been limited in the high-field imaging due to increased magnetic susceptibility and inhomogeneity artefacts. In this respect, the modified DEFT spin echo sequence appears to be an alternative to the gradient echo techniques. In this sequence, an α_x RF pulse of much smaller than $\frac{1}{2}\pi$ is applied. The rotation of the vertical component is controlled by the first π pulse for the formation of the spin echo in the transverse plane and subsequent π pulse restores longitudinal components after data acquisition. Since the RF pulse width of the π pulse for the excitation of a small object (*ca.* 2 mm) is very small, i.e. of the order of a few microseconds in three-dimensional techniques, the echo time (and thus degradation effects due to diffusion) is kept small. With the modified DEFT sequence, good T_1 contrast and substantial signal enhancement are achieved, while the inhomogeneity associated artefacts are minimal.

(*c*) *Localized high-resolution imaging in vivo using a gradient subencoding technique*

A new spatial localization technique for high-resolution imaging *in vivo* is based on convolution principles and implemented by the introduction of an additional subencoding gradient to the main phase encoding gradient (Cho & Jo 1990). Localization in the read-out direction is performed by controlling the bandwidth of the low pass filter in the receiving system. Since the free induction decay (FID) and resultant image are related by Fourier transformation, convolution of the FID with a weighting function $w(\omega_x)$ in FID domain will result in the multiplication of the selection function $W(x)$ in the image domain, i.e. on the image function $\rho(x, y)$, or

$$S'(\omega_x, \omega_y) = S(\omega_x, \omega_y) * w(\omega_x) = \mathscr{F}[\rho(x, y)\, W(x)],$$

where $w(\omega_x) = \mathscr{F}[W(x)]$, and $\mathscr{F}[.]$ and $*$ represent Fourier transform and convolution operators, respectively. The weighting function of a proper form, i.e. sinc-like function will provide a localized microscopic image $\rho(x, y)\, W(x)$ without aliasing. This method has been applied to medium large size sample, e.g. 1–2 cm diameter object instead of 1 mm diameter objects conventionally used for the microscopy.

4. Application of NMR microscopy to the cellular imaging

(*a*) *Experimental set-up*

In high-resolution NMR imaging and microscopy, the design of high field gradients and high sensitivity RF coils are major experimental considerations. For the generation of high gradient fields, a Golay-type gradient coil was developed with

PHILOSOPHICAL TRANSACTIONS OF THE ROYAL SOCIETY A MATHEMATICAL, PHYSICAL & ENGINEERING SCIENCES

cooled water circulation to prevent heat accumulation in the case of high duty cycle gradient applications (short repetition time). The gradient field strengths thus obtained were approximately 200 G cm^{-1} (0.02 T cm^{-1}) with pulse rise times of approximately 100 μs. Radio frequency coil design was based on the solenoidal coil and object and coil size were matched to maximize the filling factor (see Cho *et al.* 1988).

(*b*) *Cell lineage study*

The mechanism by which a fertilized egg becomes a complex organism remains one of the most intriguing and important phenomena in biology. For this study, it is necessary to know the normal ancestry and migration patterns of the final differentiated cells in the organism (McKay 1989). In what follows we describe some of our efforts to use NMR microscopy to help unravel some of this mystery.

The frog, *Xenopus laevis*, is a convenient and robust model system for this work. The transition from fertilized egg to tadpole takes seven to ten days. The egg is relatively large (*ca.* 1 mm diameter) and the system does not increase in volume through a significant portion of embryogenesis. Moreover, it is a well-studied system allowing comparison of NMR microscopy findings with results from other techniques (Wetts & Fraser 1989; Moody 1987). We have, therefore, applied NMR microscopy to determine normal cellular lineage patterns in *Xenopus laevis* embryos. To follow the descendants of a single cell, a lineage tracing substance is micro-injected into a single cell. Three-dimensional NMR microscopy techniques are then used to determine which cells inherit the marker.

Our initial experiments have concentrated upon demonstrating the feasibility of using NMR microscopy to obtain images *in vivo* of developing frog embryos at the requisite resolution. The fertilized egg or embryo is placed in a 2 mm internal diameter NMR tube and surrounded with low temperature gelling agar. The agar is allowed to gel, thus arresting sample movement and maintaining a moist environment. The tube is then sealed and placed in the RF coil. Fertilized eggs or embryos continue to develop after this manipulation and withstand prolonged exposure to a 7.0 T magnetic field with no obvious adverse effects.

Figure 3*a* illustrates cellular development of *Xenopus laevis* at various stages. In figure 3*b*, a cutview of the *in vivo* proton NMR microscopy images of *Xenopus laevis* embryo at a relatively late stage (*ca.* 24 h) is shown. Distinct morphological structures (e.g. neural tube) and single cell layers are readily apparent in this image. Pixel resolution is *ca.* 12 μm and slice thickness is 100 μm. The techniques shown in the previous section were used and the total data acquisition time for 16–32 slice volume imaging was *ca.* 1 h. Calculations show that these experimental conditions will yield a heavily T_1, T_2, and diffusion-weighted image where signal from 'free' water is suppressed.

The use of NMR microscopic imaging to follow cell lineages requires an injectable contrast agent. For this use we have synthesized Gd-DTPA-dextran using 20000 Dalton molecular mass dextran. It is a potent T_1 contrast agent which due to its large size should remain sequestered in a single cell and that cell's progeny. To test this hypothesis, *ca.* 50 nl of a 100 mg ml^{-1} solution of this agent were micro-injected into a single cell of a *Xenopus* blastomere at the eight cell stage. Figure 3*c* shows a slice through the centre of this embryo at the 512–1024 cell stage. Since this is a heavily T_1-weighted image, the bright areas arise from local concentrations of Gd-DTPA-dextran, i.e. daughter cells of the originally labelled cell. Most of the high intensity

PHILOSOPHICAL TRANSACTIONS OF THE ROYAL SOCIETY A MATHEMATICAL, PHYSICAL & ENGINEERING SCIENCES

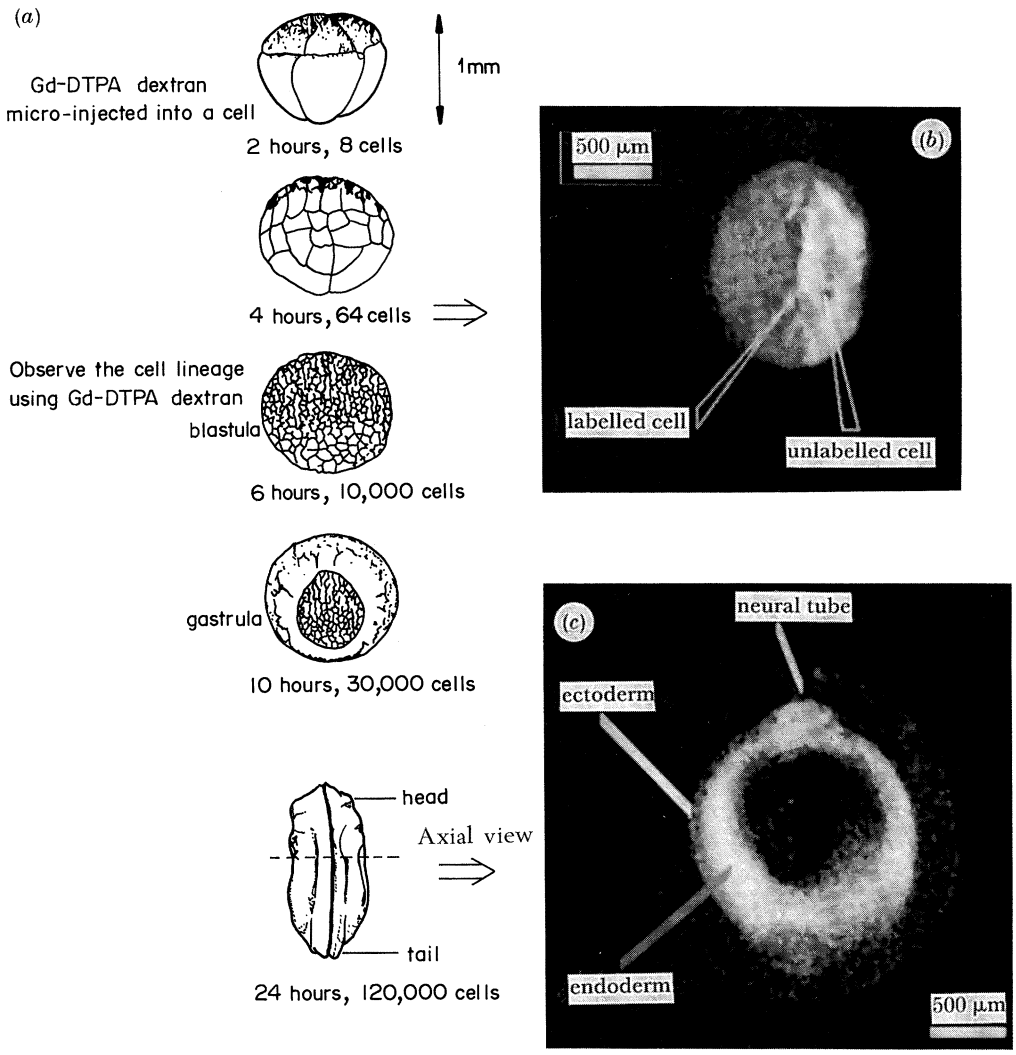

Figure 3 (*a*) An illustration of the developmental stages of a *Xenopus laevis* frog embryo. (*c*) NMR image of embryo in the early stages of neurulation obtained without contrast agent. The neural fold has not yet completely closed, thus the neural tube appears as a relatively uniform disc. (*b*) One cell in the animal pole of a *Xenopus laevis* frog embryo was injected with a solution of Gd-DTPA-dextran when it was at the eight cell stage. NMR image was recorded at the 512–1024 cell stage with the animal pole oriented to the right. Because this is a T_1-weighted image, significant intensity is to be expected only from regions in close proximity to the Gd ions.

is contiguous implying, as expected, minimal cell migration at this stage. The patches of dark within the bright area and patches of bright within the dark area are of the same size and precisely the size expected of individual cells at this stage. These images are obtained in a time shorter than the average cell division time in this system. The Gd-DTPA-dextran complex is non-toxic, membrane impermeable, and provides excellent contrast between labelled and unlabelled cells.

PHILOSOPHICAL TRANSACTIONS OF THE ROYAL SOCIETY A MATHEMATICAL, PHYSICAL & ENGINEERING SCIENCES

5. Conclusions

In this paper we have reported potentials of NMR microscopy for the study of cellular level biological samples non-invasively. These include study of ultimately attainable resolution and sensitivity with which biological sample study *in vivo* is possible. Preliminary results show that the NMR microscopy is potentially capable of providing micrometre resolution images within acceptable measurement time, which allows us to study biological samples such as embryos following various developmental steps in cellular level. Due to its non-invasive nature, it was possible to study cell lineage using NMR contrast agents (e.g. Gd-DTPA dextran) as a function of time. From this cell lineage study, NMR microscopy has demonstrated that it is not only non-invasive but is also capable of observing various time-dependent developmental steps of the embryo not easily attainable by other means.

References

Aguayo, J. B., Blackband, S. J., Schoeniger, J., Mattingly, M. A. & Hintermann, M. 1986 Nuclear magnetic resonance imaging of a single cell. *Nature, Lond.* **322**, 190–191.

Ahn, C. B. & Cho, Z. H. 1989 A generalized formulation of diffusion effects in μm resolution nuclear magnetic resonance imaging. *Med. Phys.* **16**, 22–28.

Becker, E. D., Ferretti, J. A. & Farrar, T. C. 1969 Driven equilibrium Fourier transform spectroscopy. A new method for nuclear magnetic resonance signal enhancement. *J. Am. chem. Soc.* **91**, 7784–7785.

Cho, Z. H., Singh, M. & Huth, G. C. 1978 The scanning ion microprobe: an alternative to the scanning electron microscope. *Ann. N.Y. Acad. Sci.* **306**, 223–261.

Cho, Z. H., Ahn, C. B., Juh, S. C., Lee, H. K., Jacobs, R. E., Lee, S., Yi, J. H. & Jo, J. M. 1988 Nuclear magnetic resonance microscopy with 4 μm resolution: theoretical study and experimental results. *Med. Phys.* **15**, 815–824.

Cho, Z. H. & Jo, J. M. 1990 Localized *in-vivo* high resolution NMR imaging using gradient subencoding technique. *Med. Phys.* (In the press.)

Hoult, D. I. & Richards, R. E. 1976 The signal-to-noise ratio of the nuclear magnetic resonance experiment. *J. magn. Reson.* **24**, 71–85.

Hoult, D. I. & Lauterbur, P. C. 1979 The sensitivity of the zeugmatographic experiment involving human samples. *J. magn. Reson.* **34**, 425–433.

House, W. V. 1984 NMR microscopy. *IEEE Trans. Nucl. Sci.* **NS-31**, 570–577.

Lauterbur, P. C. 1984 New direction in NMR imaging. *IEEE Trans. Nucl. Sci.* **NS-31**, 1010.

McKay, R. D. G. 1989 The origins of cellular diversity in the mammalian central nervous system. *Cell* **58**, 815–821.

Moody, S. A. 1987 Fates of the blastomeres of the 32-cell-stage *Xenopus* embryo. *Devel. Biol.* **122**, 300–319.

Wetts, R. & Fraser, S. E. 1989 Slow intermixing of cells during *Xenopus* embryogenesis contributes to the consistency of the blastomere fate map. *Development* **105**, 9–15.

PHILOSOPHICAL TRANSACTIONS OF THE ROYAL SOCIETY A MATHEMATICAL, PHYSICAL & ENGINEERING SCIENCES

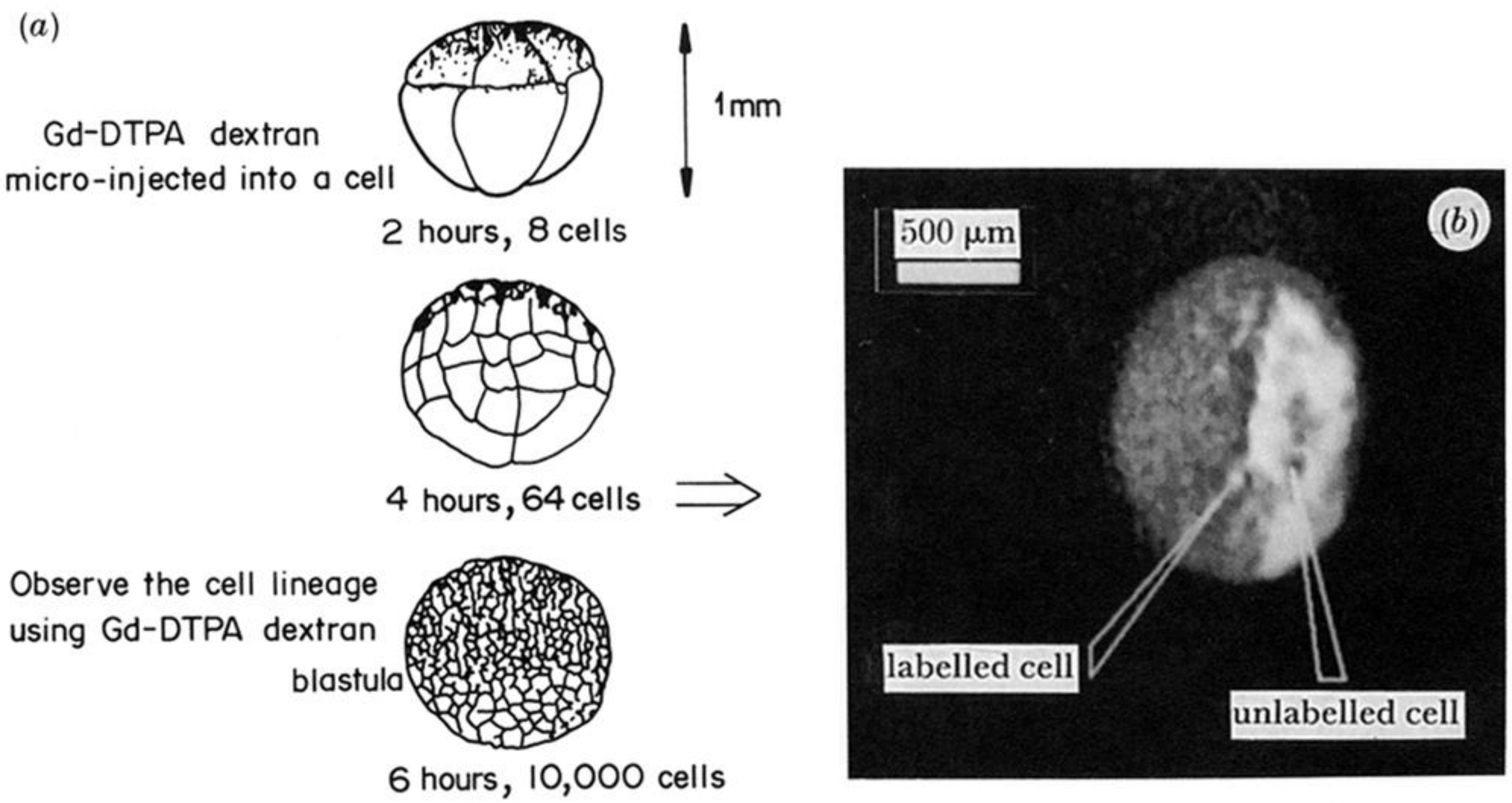

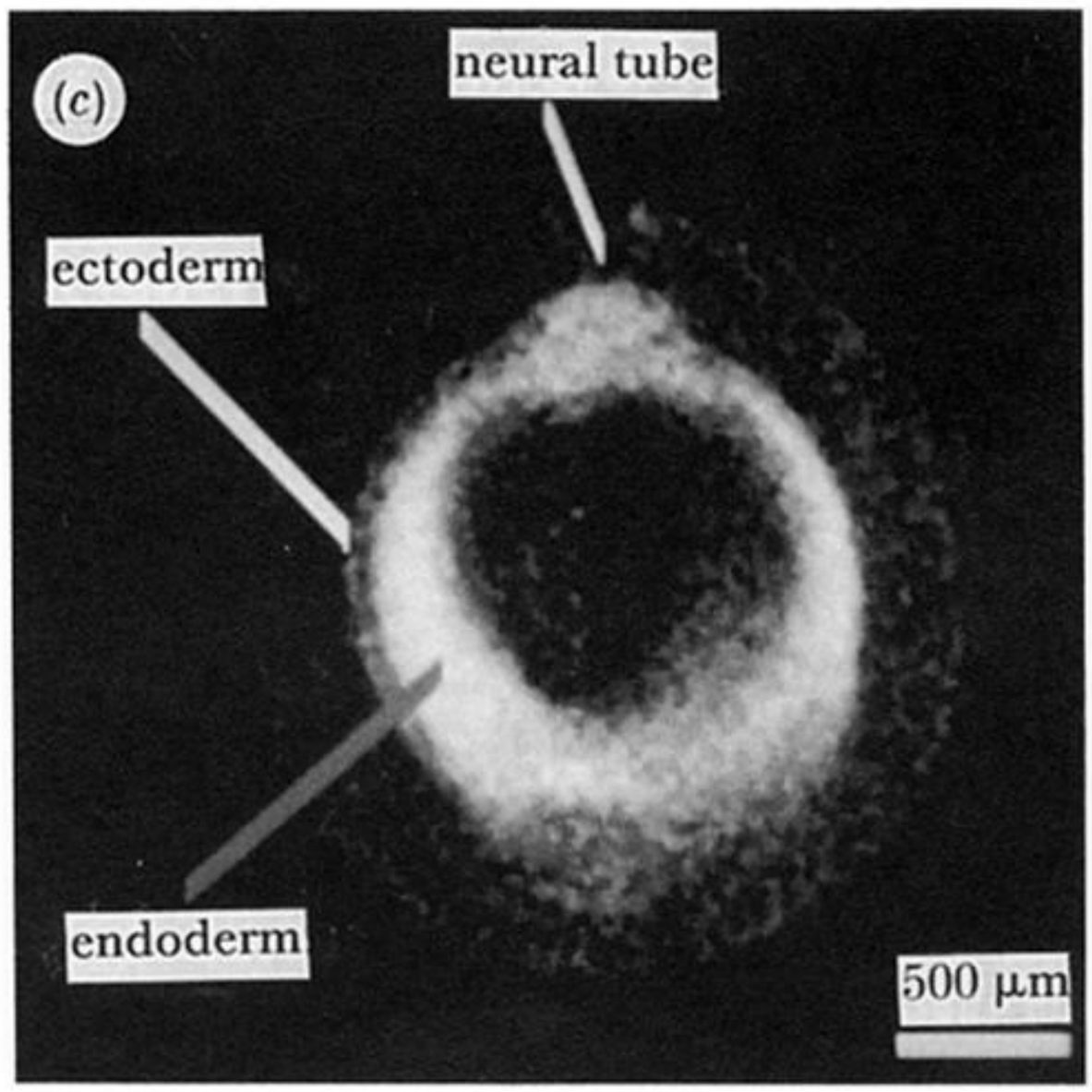

gure 3 (*a*) An illustration of the developmental stages of a *Xenopus laevis* frog embryo. (*c*) NMR nage of embryo in the early stages of neurulation obtained without contrast agent. The neural fold s not yet completely closed, thus the neural tube appears as a relatively uniform disc. (*b*) One cell the animal pole of a *Xenopus laevis* frog embryo was injected with a solution of Gd-DTPA-xtran when it was at the eight cell stage. NMR image was recorded at the 512–1024 cell stage with e animal pole oriented to the right. Because this is a T_1-weighted image, significant intensity is be expected only from regions in close proximity to the Gd ions.